Indian Journal of Chemistry
Vol. 62, July 2023, pp. 720-727
DOI: 10.56042/ijc.v62i7.3829

Synthesis of bentonite/Nano-Mn_3O_4 composite material and degradation of formaldehyde

Zhifu Wu* & Liyun Hu

Guangxi Key Laboratory of Drug Discovery and Optimization, Guangxi Engineering Research Center for Pharmaceutical Molecular Screening and Druggability Evaluation, School of Pharmacy, Guilin Medical University, Guilin 541199, China
E-mail: 1772716011@glmc.edu.cn

Received 25 October 2022; accepted(revised) 19 May 2023

In order to obtain more efficient catalytic materials for degrading the air pollutant - formaldehyde, Nano-Mn_3O_4 and bentonite / Nano-Mn_3O_4 composite catalysts (BMC) for formaldehyde degradation were prepared by sol gel method, using manganese sulfate, bentonite, citric acid and ammonia as reactants. Field emission-scanning electron microscope, Transmission electron microscope, X-ray Diffraction, Nitrogen adsorption experiments and laser particle size analyzing instrument have been employed to characterize the Mn_3O_4 and BMC nanoparticles, respectively. The mechanism and effect of formaldehyde degradation of these substances are also discussed. The results show that BMC catalytic material has a better ability to degrade formaldehyde in air than Mn_3O_4 at the room temperature, which is resulted by the strong adsorption capacity of bentonite providing a reaction site and molecular collision site for oxidative decomposition of formaldehyde. And the synthesized catalytic materials have the advantages of low cost, easy regeneration and recycling.

Keywords: Bentonite, Nano-Mn_3O_4, Formaldehyde pollution, Catalytic degradation, Composite material

Bentonite has the characteristics of large reserves and low price, and has excellent adsorption performance and ion exchange performance. It is widely used in petroleum, chemical, paper, food, drilling, agriculture, pharmaceutical, ceramics and other industries. It is often praised as "universal material"[1-3], especially as adsorbents with important value in the field of environmental protection and medicine. The structure of bentonite consists of two layers of silicon-oxygen tetrahedron and one layer of aluminum-oxygen octahedron. Si^{4+} in tetrahedron can be replaced by Al^{3+}, and Al^{3+} in octahedron can be replaced by Fe^{2+}, Zn^{2+}, Mn^{2+}, Li^{+}, *etc*. Negative charge between layers is formed. After lattice replacement, bentonite has the ability to adsorb cations. Inserting metal oxides into the middle of bentonite layer is one of the important methods to modify its properties[4]. Formaldehyde is the main harmful pollutant in indoor air, which is irritating and carcinogenic to the human body, and is recognized as one of the human carcinogens by the International Agency for Research on Cancer[5]. When the indoor formaldehyde concentration exceeds 0.10 mg/m^3, you can smell peculiar smell. When it exceeds 0.50mg/m^3, it will irritate the eyes and cause tears. When the formaldehyde concentration exceeds 30 mg/m^3, it can lead to death. Furniture, adhesives, fresheners, cosmetics, *etc*. are the main sources of indoor formaldehyde. Common methods for removing formaldehyde mainly include opening doors and windows for ventilation, indoor cultivation of plants, activated carbon adsorption and catalytic oxidation[6,7]. In recent years, many scholars have found that mixed-valence-state metal oxides, such as Mn_3O_4, can catalyze the decomposition of formaldehyde in the air at room temperature[8,9]. Wang M *et al.*[10] have prepared MnO_x-CeO_2 catalyst to degrade formaldehyde, which showed excellent formaldehyde oxidation activity. Kang Z.W *et al.*[11] have prepared an autonomous driving friction electrocatalyst for a three-dimensional nanocomposite structure by using an electrospinning and hydrolysis reaction, which promotes the generation of reactive oxygen species and promotes the degradation of formaldehyde. Wang M.K *et al.*[12] have performed photocatalytic degradation of toluene gas using porous Mn_3O_4 doped TiO_2, and they have found a high catalytic efficiency[13]. Although many highly active MnO_2 catalysts have been successfully synthesized, they cannot be directly used in practical application and are usually loaded on the carrier in the form of particles for subsequent catalytic oxidation[14]. Therefore, it is

particularly important to find new carriers for supporting catalysts. According to literature research, there is rare report on the preparation of manganese tetroxide and BMC by sol-gel method[15]. In this paper, the nanoscale Mn_3O_4 and BMC were synthesized by this method, and the specific surface area of these two products and their degradation effect on formaldehyde in the air were tested, and then their catalytic mechanism was explored.

Experimental Section

Experimental reagents and instruments

Bentonite (CP, Nanjing Chemical Reagent Co., Ltd.), citric acid (AR, Tianjin Fuyu Fine Chemical Co., Ltd.), $MnSO_4$ (AR, Tianjin Chemical Reagent No. 1 Factory), $NH_3 \cdot H_2O$, $NH_4Fe(SO_4)_2$, HCHO and Phenol reagent (3-methyl-2-benzothiazolinone hydrazone hydrochloride hydrate)(AR) were purchased from Nanjing Chemical Reagent Co., Ltd.), Deionized water. Box type resistance furnace (Shenyang Energy Saving Electric Furnace Factory) and Vacuum Dryer (Shanghai Suopu Instrument Co., Ltd.) were used in the preparation process. The X-ray diffraction (XRD) patterns were recorded on a UItima III diffractometer (Japan Rigaku Corporation) with Cu-K_α radiation at a scanning speed of 4°/min from 10 to 70°. Field emission scanning electron microscope (FE-SEM) were performed on a Regulus 8100 (Hitachi, Japan) coupled with energy dispersive X-ray spectroscopy (EDS), the accelerating voltage and applied current were 40 kV and 30 mA, respectively). Transmission electron microscope analysis was conducted with a JEOL, JEM2100PLUS (Japan Electronics Co., Ltd.) microscope operated at 200 kV. The samples were dispersed in ethanol and deposited on Cu grids prior to observation. Nitrogen adsorption/desorption isotherms at –195.85°C were measured on a Micromeritics TriStar 3000 instrument. All samples were outgassed at 150°C for 12 h under flowing N_2 before the measurement. The specific surface areas were calculated by the Brunauer–Emmet–Teller (BET) methods. The particle size and particles size distribution were examined on a laser particles size analyzing equipment (Mastersizer 2000, England). Xuzhou Xingke 6-in-1 formaldehyde tester was used to detect the concentration of HCHO.

Synthesis of (BMC) materials

Synthesis of Nano-Mn_3O_4

According to the φ-*p*H relationship shown in Fig. 1, there are two main ways to prepare Mn_3O_4 in the wet

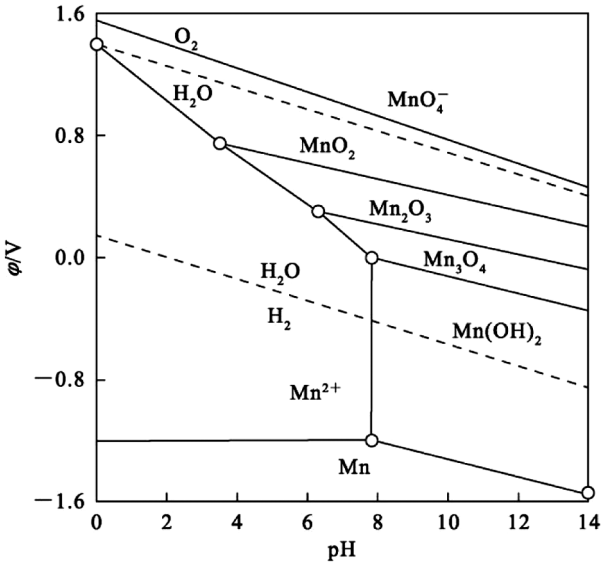

Fig. 1 — The φ-*p*H relationship diagram of manganese

process: 1)Direct oxidation ofMn^{2+} to generate Mn_3O_4, referred to as one-step oxidation method; 2) Mn^{2+}first generates$Mn(OH)_2$, and then obtainsMn_3O_4 by oxidation, referred to as two-step oxidation[16,17]. The one-step oxidation process is short and the cost is low, but the *p*H, temperature, surfactant, *etc*. of the solution system have a great influence on the formation and microstructure of particles.

The schematic illustration of synthesis process is shown in the Fig. 2. Bentonite is a lamellar structure composed of Si-O tetrahedral and Al-O octahedral, in which the tetrahedral are connected to each other with three top angles in the same plane, forming a grid with hexa square symmetry. The octahedron is composed of an aluminum, magnesium and other cation between two hydroxide and iron ions. There are H^+, Na^+, Ca^{2+} between the lamellae, which are easily displaced to insert into inorganic or organic molecules. Therefore, the as formed Mn_3O_4 intercalation is also possible within the layered structure. Apart from that, the surface morphological images reveals that some of the Mn_3O_4 were also formed on the surface of the sodium bentonite clay which confirm that the as formed product is BMC in addition to the manganese oxide intercalation process[18,19].

The typical preparation process was as follows: 1.89g of citric acid and 0.64g of manganese sulfate according to the amount of the substance 2:1 in the beaker, added an appropriate amount of deionized water to make it dissolved, then added $NH_3 \cdot H_2O$ to adjust *p*H to 8. The beaker was placed in an electric thermal drying box, heated to 80°C for 5 hours before

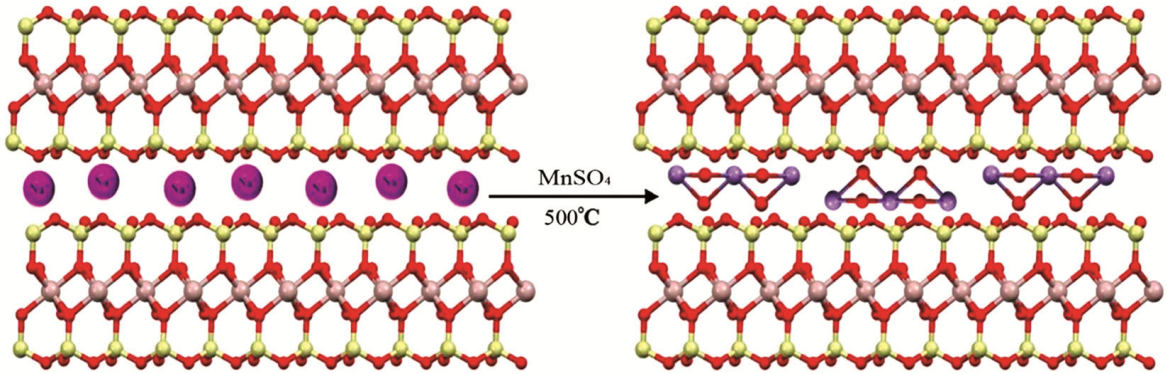

Fig. 2 — Schematic illustration for the formation of BMC

the solution becomes gel, further heated to 120°C and dried for 6 hours, and the wet gel became dry gel. After cooling, the dry gel was removed and ground into a powder, transferred the powder to the crucible, put into a high temperature furnace, heated from RT to 500°C for 3 hours, then cooled to RT, and thus the product was obtained.

Synthesis of BMC materials

BMC was synthesized by repeating the above experimental procedures by adding 2 g fully dried activated bentonite to the reactant for preparing Mn_3O_4 composite powder.

Experimental method for degradation of HCHO at RT

50 mL of formaldehyde solution was placed in a vacuum desiccator for 4 hours until gas-liquid equilibrium, then 0.135g catalyst was added from the upper orifice into the desiccator. The concentration of formaldehyde was measured after half an hour in the other outlet of desiccator. The Phenol Reagent Spectrophotometry is used which is the method for the determination of formaldehyde in the air of public places (GB/T18204.26-2000). Formaldehyde concentration was measured every half an hour during the whole process.

Results and Discussion

Phase analysis

Fig. 3 illustrates the XRD patterns of BMC, from which it can be seen that, it is mainly composed of two phases. The diffraction peaks locate at 2θ values of 17.9°, 28.7°, 30.8°, 32.3°, 36.1°, 44.4°, 50.9°, 56.0°, 58.4°, 59.9° and 64.5° corresponding to the characteristic peaks of the JCPDS standard card PDF # 75-1560, which indicates

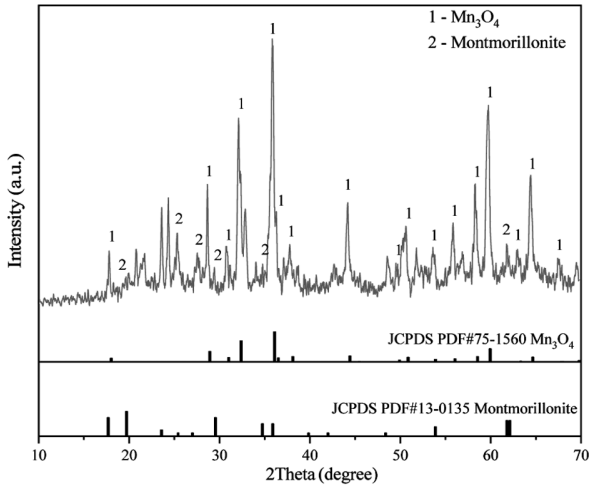

Fig. 3 — XRD pattern of BMC

that the sample mainly contains Mn_3O_4. The diffraction peaks at 2θ values of 20.0°, 25.5°, 34.9° and 61.9° coincide with the JCPDS standard card PDF # 13-0135. Therefore, the synthesized sample contain bentonite and Mn_3O_4. Other unexpected peaks belong to the diffraction of manganese sulfate, but this substance has no effect on the catalytic properties.

SEM images and EDS analysis

The size and morphology of the products synthesized were observed by SEM, while element content was quantified using EDS. Fig. 4 presents the typical SEM images of Mn_3O_4, bentoniteand BMC. It can be seen from Fig. 4a,b that the products are composed of a large quantity of near spheres with diameter of 150−250 nm. An interesting feature is that each sphere is constructed by many smaller particles with size of 15−25 nm. The little spheres are loose and very rough. Fig. 4 c,d show the SEM images of bentonite flake structure. It can be seen that these

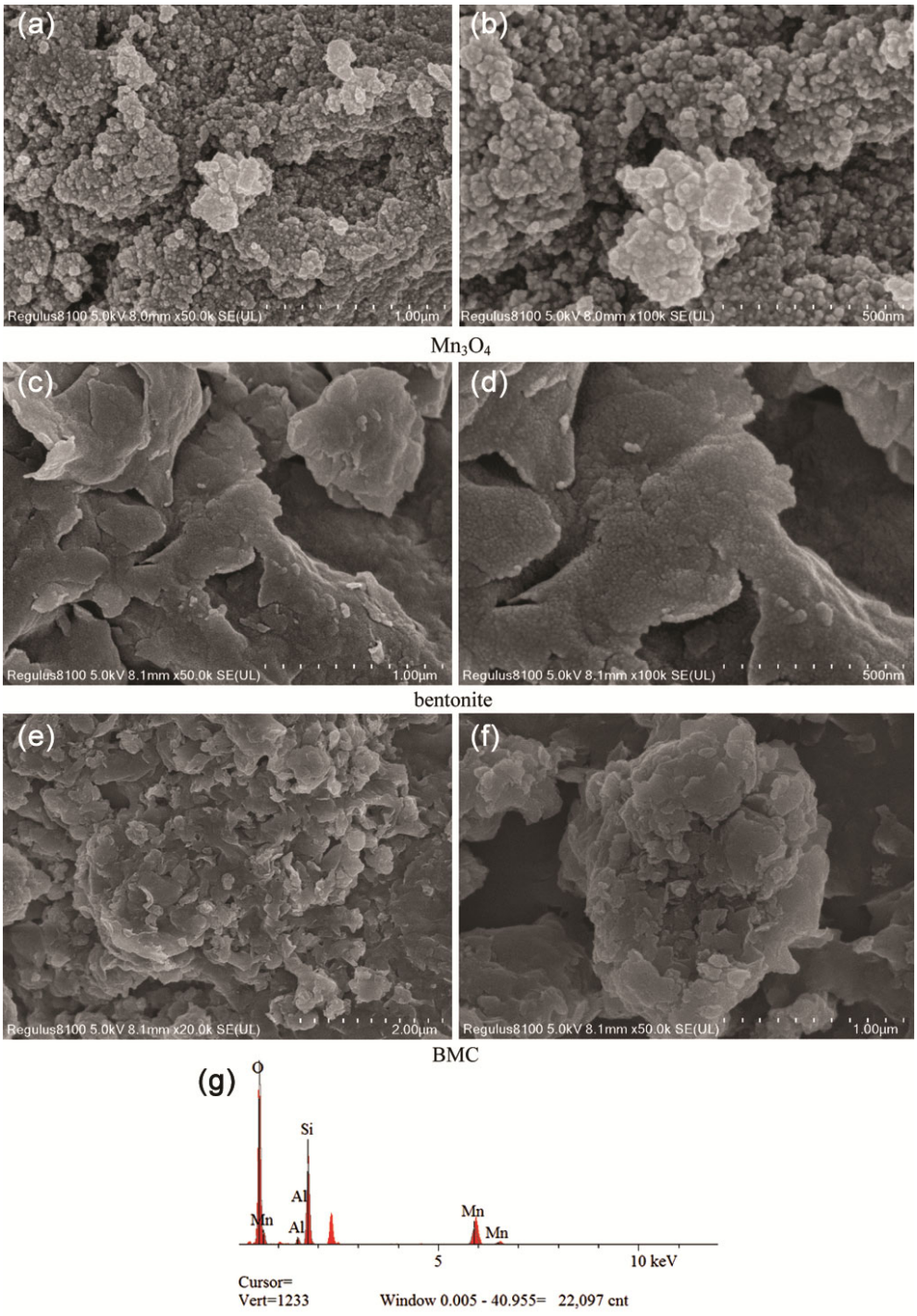

Fig. 4 — SEM images and EDS analysis

sheet particles have no regular geometry shape, and the size of the contour is about 200 nm to 1 μm, and the thickness is about 50 nm. It can be clearly seen from Fig. 4e,f that the spherical nanoparticles are firmly embedded in the middle of the flake particles. Combined with the EDS results, Fig. 4g it can be inferred that the nano-manganese oxide is inserted between the layers of bentonite to form BMC. The element content was quantified using EDS. Compositional properties of the samples are summarized in the Table 1, while selected SEM images are given in Fig. 4f.

Table 1 — The element content of BMC

Element	Atomic %	Content wt.%
O	56.94	32.37
Al	1.31	1.25
Si	15.85	15.82
Mn	25.91	50.56

TEM images

Fig. 5a,b show the TEM images of nano-manganese oxide. Clearly, the particles exhibit closely to the monodisperse sphere with average diameter of 23.7 nm as measured by the software Image J. Fig. 5c,d show the TEM images of bentonite, it can be seen that the products are composed of many

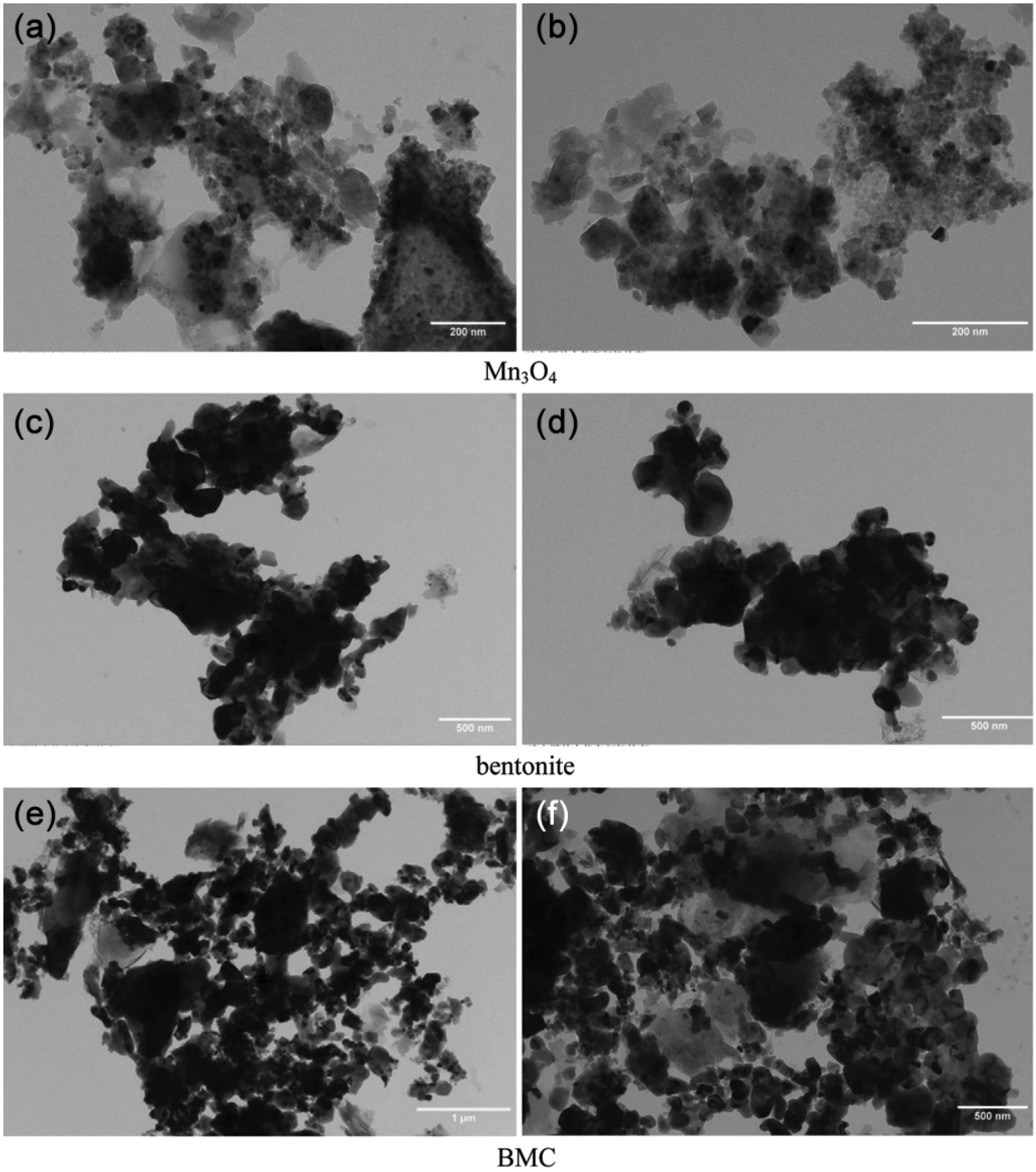

Fig. 5 — TEM images

sheet stacking structures. Fig. 5e,f show the TEM images of the BMC. The particle size shown in the figure can be divided into two parts. One part is mostly nanoparticles with an average diameter of 260 nm, and the other part is mostly with an average diameter of 140 nm. It is speculated that most of the Mn_3O_4 and bentonite are compounded together, but there are also monomers, showing polarization.

Fig. 6 shows the results of the nanoparticle analyzer. The particle size of Mn_3O_4 is mainly distributed in the range of 90-220 nm, and the particles with a diameter of 141 nm are the most. The particle size of bentonite is mainly distributed in the range of 141-256 nm, and the particles with a diameter of 190 nm are the most, which is consistent with TEM.

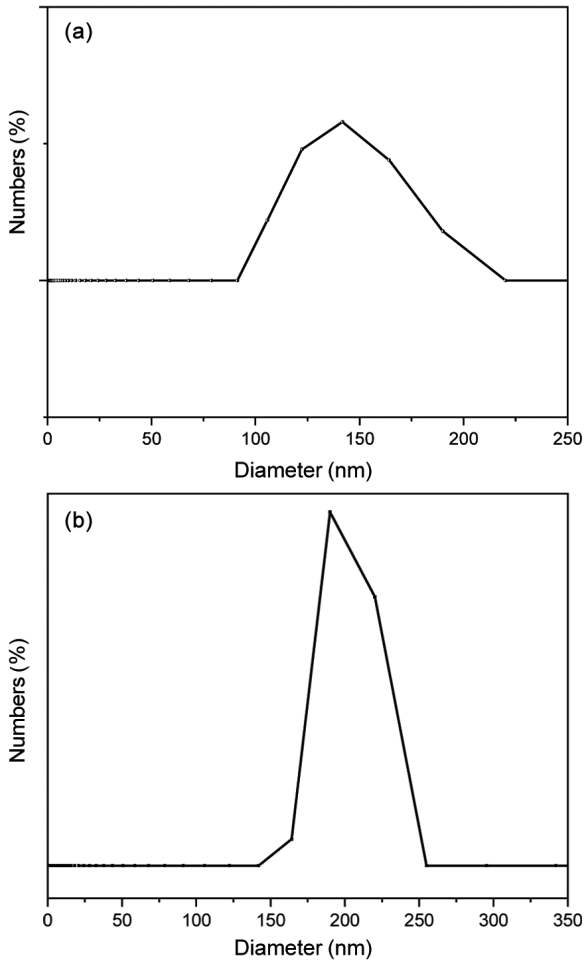

Fig. 6 — Size distribution diagram (a: Mn_3O_4 , b: BMC)

Results and mechanism of formaldehyde degradation

Table 2 shows the experimental results of the degradation of formaldehyde by Mn_3O_4 and BMC. As can be seen from the table, after half an hour of reaction, the degradation rate of formaldehyde was 61.5% and 76.9% respectively; After 2.5 hours of reaction, the concentration of formaldehyde degraded by nano-Mn_3O_4 decreased to 0.025mg/m^3, and the concentration of formaldehyde degraded by BMC decreased to 0.012 mg/m^3.

This shows that although both catalysts have the ability to degrade formaldehyde, BMC is more effective than Mn_3O_4. This is because Mn_3O_4 directly catalyzes the oxidation and degradation of formaldehyde, while bentonite with Mn_3O_4 has a fluffy and porous structure, which can not only provide reaction sites for Mn_3O_4, but also adsorb aggregated formaldehyde gas, which greatly increases the collision rate between formaldehyde gas and oxygen free radicals, and is conducive to the catalytic oxidation and degradation of formaldehyde by Mn_3O_4 and reduces its concentration.

Nitrogen isothermal adsorption

Nitrogen adsorption method is one of the important and effective means to study the structural characteristics of porous materials, adsorption isotherm is a specific description of the adsorption phase equilibrium, by determining the type of adsorption isotherm, and then determine the essence of the adsorption process, so that people can better understand various adsorption mechanisms, but also can obtain the specific surface area, pore volume, pore size distribution and other information of the material, so as to provide a theoretical basis for the application of the material.

Fig. 7 shows the nitrogen adsorption isotherm of BMC. The solid line (a) is the adsorption curve and the dashed line (b) is the desorption curve. With the change of pressure, the nitrogen adsorption capacity of the sample shows different characteristics. The

Table 2 — Comparison of HCHO degradation results between pure Mn_3O_4 and BMC

Reaction time (h)	0	0.5	1	1.5	2	2.5
HCHO content after pure Mn_3O_4 degradation（mg/m^3)	0.39	0.15	0.07	0.051	0.031	0.025
HCHO content after degradation of BMC（mg/m^3)	0.39	0.09	0.06	0.036	0.017	0.012

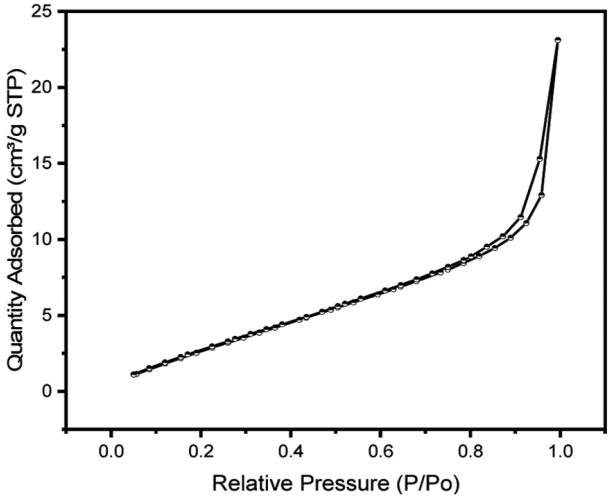

Fig. 7 — Nitrogen adsorption isotherms linear plot of BMC

nitrogen adsorption isotherm of the sample is complex and meaningful. It is difficult to attribute it to the simple Class 5 isotherms of BDDT divided by the early Brunauer. Instead, it belongs to IUPAC class 6 isotherms carry type V, with a residual loop of H_3 compression type. In the third H_3 case, the adsorption branch curve of the retained loop does not show the ultimate adsorption capacity at higher relative pressure, and the adsorption capacity increases monotonically with the increase of pressure. This is mostly found in sheet materials with narrow tear-type pore structures[20,21]. From the BET (Brunauer-Emmett-Teller) equation, the specific surface area of the material can be calculated as 22.3345m^2/g, Langmuir has a surface area of 348.7612m^2/g.

According to the above theory, the isotherm can be explained in two segments. The first part, during the adsorption process, begins at a lower pressure, when the relative pressure is less than 0.75, the adsorption of adsorbate gas is monolayer adsorption and the adsorption and desorption curves are combined into one. The second part, as the pressure increases, begins to transform into multilayer adsorption. When the relative pressure is greater than 0.75, the adsorption capacity of N_2 increases rapidly with the increase of relative pressure, and a retention loop occurs. This is due to the decrease of pore size caused by multi-layer adsorption, the capillary condensation of adsorbed gas occurs, and finally the liquid is formed. While in the process of desorption, the morphology of the phase interface changed, so the desorption curve is separated from the adsorption curve forming a retention loop.

Fig. 8 and Fig. 9 show the data on the pore size and pore volume of BMC. The data in Figure clearly

Pore Size	
Adsorption average pore diameter (4V/A by BET):	9.0459 nm
Desorption average pore diameter (4V/A by BET):	5.3480 nm
BJH Adsorption average pore diameter (4V/A):	15.5567 nm
BJH Desorption average pore diameter (4V/A):	13.9696 nm
D-H Adsorption average pore diameter (4V/A):	10.2183 nm
D-H Desorption average pore diameter (4V/A):	11.0479 nm
Horvath-Kawazoe	
Maximum pore volume at P/Po = 0.175117920:	0.003422 cm³/g
Median pore width:	0.8683 nm

Fig. 8 — Data on pore size of BMC

Pore Volume	
Single point adsorption total pore volume of pores less than 220.3518 nm diameter at P/Po = 0.991235160:	0.050509 cm³/g
Single point desorption total pore volume of pores less than 40.3122 nm diameter at P/Po = 0.950000000:	0.029861 cm³/g
t-Plot micropore volume:	-0.007093 cm³/g
BJH Adsorption cumulative volume of pores between 2.1505 nm and 300.0000 nm diameter:	0.047908 cm³/g
BJH Desorption cumulative volume of pores between 2.3123 nm and 300.0000 nm diameter:	0.048532 cm³/g
D-H Adsorption cumulative volume of pores between 1.7000 nm and 300.0000 nm diameter:	0.054917 cm³/g
D-H Desorption cumulative volume of pores between 1.7000 nm and 300.0000 nm diameter:	0.059213 cm³/g

Fig. 9 — Data on pore volume of BMC

shows the average pore size and pore volume of the composite powder. The bentonite is a kind of sheet shaped material, where the holes are made of the sheet particles accumulation, it is not regular.

Catalytic mechanism discussion

The mechanism of Mn_3O_4 degradation of HCHO is described by previous papers[22,23]. Firstly, free oxygen molecules in gas phase could be captured by oxygen vacancies on the surface of the catalyst and then stripped and decomposed into active oxygen species (radicals) under the action of Mn_3O_4. Secondly, the oxygen radicals collide with the adsorbed HCHO on the catalyst surface coming into carbon dioxide and hydrogen radicals. Thirdly, hydrogen radicals combined with oxygen radical to generate water. The reaction equation is summarized as follows:

$$O_2 \xrightarrow{Mn_3O_4} 2\cdot O \quad (1)$$

$$HCHO + \cdot O \longrightarrow CO_2 + 2\cdot H \quad (2)$$

$$2\cdot H + \cdot O \longrightarrow H_2O \quad (3)$$

In the process of oxidation, Mn_3O_4 plays a catalytic role accelerating the process of the oxidation reaction, and eventually oxidize the formaldehyde into water and carbon dioxide. The adsorption ability of bentonite itself increases the concentration of formaldehyde around Mn_3O_4, thus speeding up the catalytic oxidation of formaldehyde by Mn_3O_4, and the two play a synergistic effect.

Conclusion

In conclusion, Nano-Mn_3O_4 and BMC have successfully synthesized by sol-gel method without using any hazardous chemicals. The results show that both the products have ability to catalyze formaldehyde in air, but the BMC is superior to Mn_3O_4, which is caused by the strong adsorption capacity of bentonite. It can provide a reaction site and molecular collision site for formaldehyde degradation[24,25]. In addition, the synthesized catalytic materials have the advantages of low cost, easy regeneration and recycling.

Acknowledgments

This work was supported by the Foundation of Guilin Medical University for doctoral research project (112019071).

References

1 Elgarhy A H, Mahran B N A, Liu G, Salem T A, ElSayed E E &Ibrahim L A, *Sci Rep*, 12 (2022) 19433.
2 Zhang Y, Zhu Y M, Ren Q &Jiang Z W, *J Chin Ceram Soc*, 50 (2022) 420.
3 Liu G, Xu L S, Li Z K, Huang Q Q, Xie Z W&Xu X F, *J Chin Ceram Soc*, 46 (2018) 1414.
4 Peng X D, Liu H, Qin X, Zhou Y D & Fe T, *J Chin Ceram Soc*, 42 (2014) 514.
5 Soltanpour Z, Yousef M & Yadolah F, *Environ Res*, 204 (2022) 112094.
6 He T, Zhou Y, Ding D & Rong S,*ACS Appl Mater & Interfaces*, 13 (2021) 29664.
7 Abubakar Y, Sun Y, Liu S, Wang C, Ren Y, Xiao H, Snape C & He J, *J Hazard Mater*, 424 (2022) 127583.
8 Sidheswaran M A, Destaillats H, Sullivan D P, Larsen J & Fisk W J, *Appl Catal B-Environ*, 107 (2011) 34.
9 Ahmed K A M, Zeng Q, Wu K &Huang K, *J Solid State Chem*, 183 (2010) 744.
10 Wang M, Hong X W, Chen J J, Li J, Chen X P, Mi J X, Liu Z M & Xiong S C, *Chem Eng J*, 440 (2022) 135854.
11 Zhao W K, Zheng J Y, Han C B, Ruan J, Lu Y G, Zhou K L, Zhai T R, Wang H &Yan H, *Chem Eng J*, 440 (2022) 135877.
12 Jothiramalingam R & Wang M K, *J Hazard Mater*, 147 (2007) 562.
13 Sekine Y & Nishimur A, *Atomospheric Environ*, 35 (2001) 2001.
14 Qu Y S, Zheng X M &Ma K K,*Chem Eng J*, 430 (2022) 132954.
15 Hua J, *J Environ Chem Eng*, 6 (2017) 156.
16 Nong Y Y, Li C L, Ruan J, Yang M F, Wang W H, Yan G J & Liao W F, *Hydrogometallurgy China*, 41 (2022) 34.
17 Jia H & Zhao Z, *Inorg Chem Ind*, 46 (2014) 45.
18 Bama K & Sundrarjan M, *Res Chem Intermed* , 43 (2017) 2351.
19 Bachra Y, Grouli A, Damiri F, Zhu X X, Talbi M & Synthesis M B, *ACS Omega*, 7 (2022) 39002.
20 Rouquerol J, Avnir D, Falrbridge C W, Everett D H, Haynes J M, Pernicone N, Ramsay J D F, Sing K S W & Unger K K, *Pure Appl Chem*, 66 (1994) 1739.
21 Du J Q, Zhsng Y, Tian T, Yan S C &Wang H T, *Mater Res Bull*, 44 (2009) 1347.
22 Zhou X Y, Zhang P, Jiang W, Yang Y T,Ling L L & Zhang W ,*Chi J Environ Eng*, 9 (2015) 5965.
23 Sekine Y, *Atmospheric Environ*, 36 (2002) 5543.
24 Zhou H W, Perreault W E, Mukherjee N & Zare R N, *Science*, 374 (2021) 960.
25 Wang X A & Yang X M, *Science*, 374 (2021) 938.